International Journal of Environmental Sciences
ISSN: 2229-7359
Vol. 10 No. 6s,2024
https://theaspd.com/index.php

Adaptive Frequency Reconfigurable Multiband Microstrip Antenna Employing Fractal Ground Geometry For Advanced Wireless Applications

Surya Bhushan Dubey[1], Kamal Prakash Pandey[2], Rakesh Kumar Singh[3], Santosh Dubey[4], Saiyed Salim Sayeed[5], Amrees Pandey[6*]

[1]Department of Electrical and Electronics Engineering, S. R. Institute of Management and Technology, Lucknow, Uttar Pradesh, India
[2]Department of Electronics and Communication Engineering, BBS College of Engineering and Technology, Prayagraj, Uttar Pradesh, India
[3, 6]Department of Electronics and Communication Engineering, Shambhunath Institute of Engineering and Technology (SIET), Prayagraj, Uttar Pradesh, India
[4]Department of Electronics and Communication Engineering, United College of Engineering and Research (UCER), Prayagraj, Uttar Pradesh, India
[5]Department of Electronics and Communication Engineering, Institute of Technology and Management, Maharajganj, Uttar Pradesh, India
suryadubey1@gmail.com[1], pandeykamal.1976@gmail.com[2], rksingh_rakesh@yahoo.com[3], sdubeyece@gmail.com[4], saiyedsalimsayeed@gmail.com[5], amrishpandey19@gmail.com[6]
[*]**Corresponding Author Email:** amrishpandey19@gmail.com

Abstract: *This work presents a frequency-reconfigurable microstrip patch antenna capable of operating at multiple resonant modes. In the OFF state, the antenna resonates at 8.17, 11.13, 15.77, and 17.46 GHz, while in the ON state it achieves resonances at 8.38, 11.13, 14.51, 16.20, 17.46, and 18.52 GHz. The reconfigurability is enabled through a single PIN diode, modeled and analyzed using HFSS, ensuring reliable switching between bands. The design covers both X-band (8–12 GHz) and Ku-band (12–18 GHz), making it suitable for modern multiband wireless communication. To enhance performance, square fractal slots are etched into the ground plane, resulting in improved bandwidth and gain characteristics. The antenna is realized on a low-cost FR-4 substrate (ε_r = 4.4, thickness = 1.6 mm). Simulation results confirm significant improvements in return loss, stable radiation patterns, and higher gain, demonstrating the antenna's potential for advanced reconfigurable wireless systems.*

Keywords: *Reconfigurable Antenna, Fractal Ground, PIN Diode, Return Loss, VSWR, Radiation Efficiency, Multiband Communication.*

1. INTRODUCTION

Microstrip patch antennas have long been recognized as a fundamental element in wireless communication systems due to their low profile, ease of fabrication, and compatibility with planar and integrated circuits [1]. Over the years, a wide range of design techniques have been developed to enhance their performance and meet the growing demands of modern wireless applications. The primary design objectives have generally focused on achieving higher gain, broader bandwidth, and better radiation efficiency [2]. Among the most recent advancements, the incorporation of fractal geometries and reconfigurability has gained significant attention [3]. Several design strategies such as the use of defective ground structures (DGS), slotted patches, and fractal geometries have been reported to improve the overall antenna performance [4]. Fractal geometries, characterized by properties like self-similarity and space-filling, consist of scaled-down repetitive structures, enabling compact designs with wideband or multiband characteristics [5–6]. For instance, the introduction of fractal-shaped slots in the ground plane has demonstrated considerable improvements in bandwidth, in some cases by up to 3.5 times the original value [7]. Additionally, the integration of different fractal geometries can lead to effective miniaturization by lowering the resonant frequency, thereby reducing the overall antenna size without compromising performance [8–9].

In present-day wireless systems, there is a growing demand for antennas that are compact, cost-effective, multifunctional, and capable of supporting multiple standards simultaneously. This requirement can be effectively addressed by merging fractal geometries with reconfigurable techniques [10–11]. Antenna reconfigurability, particularly frequency reconfiguration, allows the antenna to dynamically switch between multiple operating bands, thereby enabling its use in diverse applications [12–13]. Recent works have demonstrated innovative methodologies that combine fractal designs with reconfigurable techniques, resulting in antennas that not only provide enhanced bandwidth and miniaturization but also ensure operational flexibility across different frequency ranges [14–15]. Reconfigurable microstrip patch antennas are typically realized by incorporating switching devices such as PIN diodes, varactors, MEMS switches, or optical switches into the radiating structure [16–17]. These devices enable selective connection and disconnection of specific sections of the patch or ground plane, thereby redistributing the surface current and altering the resonant modes of the antenna [18]. Such switching-based reconfiguration offers a reliable mechanism for achieving dynamic frequency tuning and improving the adaptability of antennas in evolving wireless environments [19]. Motivated by these advancements, this paper presents the design and analysis of a frequency-reconfigurable microstrip patch antenna incorporating a fractal ground structure for bandwidth enhancement and multiband operation. The proposed design leverages PIN diode switching to achieve frequency reconfigurability while simultaneously exploiting the advantages of fractal geometries to enhance bandwidth and gain, making it a promising candidate for next-generation wireless communication systems [20]. Figure 1 illustrates two fundamental aspects of antenna reconfiguration: the techniques employed to achieve reconfigurability and the optimization parameters that dictate antenna performance. Depending on the design requirements and intended applications, different reconfiguration methods can be utilized. Among them, electrical reconfiguration is the most widely adopted approach, where switching devices such as PIN diodes, varactor diodes, or RF MEMS are integrated into the antenna structure. These devices dynamically modify the surface current distribution, enabling changes in operating frequency, polarization, and radiation pattern. Optical reconfiguration makes use of photoconductive materials or optical switches that alter the electrical properties of the antenna upon illumination. Mechanical reconfiguration involves physically modifying the geometry by rotating, sliding, or deforming the radiating elements to achieve tunability. Furthermore, material-based approaches, such as the use of liquid crystals, ferrites, and metamaterials, provide flexible control over dielectric or magnetic properties, enabling efficient frequency tuning and polarization agility [21–22].

The effectiveness of reconfigurable antennas largely depends on several optimization parameters. Return loss and VSWR are essential for impedance matching and minimizing reflection losses, ensuring efficient power transfer. Radiation pattern, gain, and directivity determine the antenna’s ability to focus and direct radiated energy, while bandwidth governs its suitability for multiband or wideband operation. Additionally, radiation efficiency is critical for evaluating how effectively input power is converted into radiated electromagnetic waves. Proper optimization of these parameters leads to enhanced adaptability, compact size, and multifunctional capabilities, making reconfigurable antennas highly attractive for modern communication systems such as 5G, IoT, and satellite networks [23–24].

International Journal of Environmental Sciences
ISSN: 2229-7359
Vol. 10 No. 6s,2024
https://theaspd.com/index.php

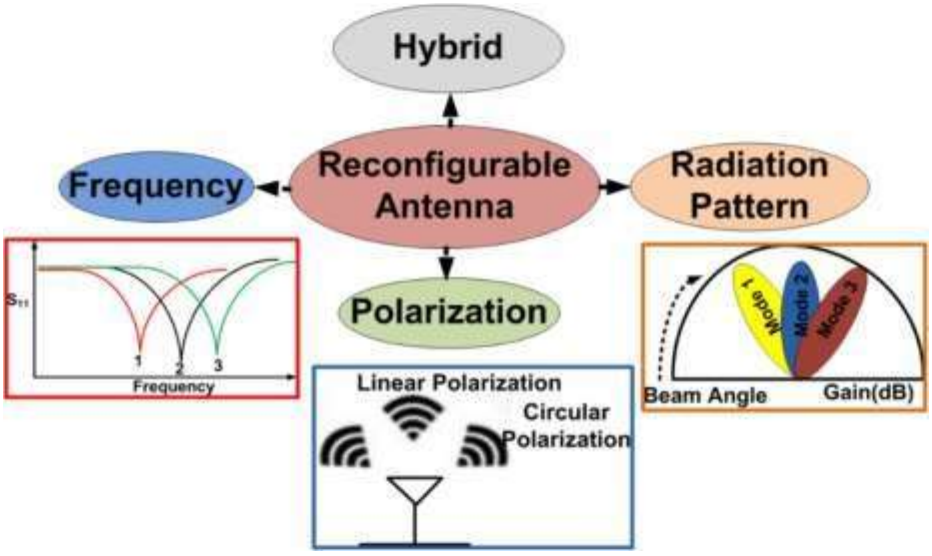

(a)

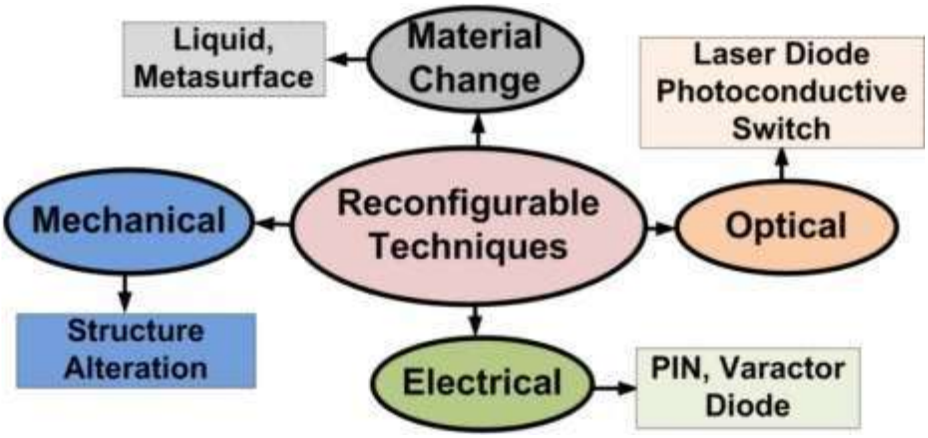

(b)

Fig. 1: (a) Various techniques employed for antenna reconfiguration and (b) Key optimization parameters influencing antenna performance.

Reconfigurability is generally realized through various switching mechanisms, including PIN diodes, RF MEMS, varactor diodes, lumped elements, and capacitive switches [25]. Among these, PIN diodes and varactor diodes are particularly favored because of their fast switching speed, ease of integration, and low cost. Specifically, PIN diodes offer switching speeds in the range of 1–100 ns, making them highly suitable for real-time and dynamic frequency reconfiguration in advanced wireless systems [26-27].
Numerous studies have validated the efficiency of these switching techniques in enabling both frequency and pattern reconfigurability. Antennas integrated with PIN or varactor diodes have demonstrated the ability to operate across multiple frequency bands while maintaining table radiation characteristics, thereby proving to be reliable and versatile solutions for next-generation wireless communication applications [28-29].

2. GEOMETRICAL FRAMEWORK AND EVOLUTIONARY STAGES OF THE PROPOSED ANTENNA

International Journal of Environmental Sciences
ISSN: 2229-7359
Vol. 10 No. 6s,2024
https://theaspd.com/index.php

The proposed antenna design is developed through multiple stages of systematic optimization, as illustrated in Figures 2 and 3. Initially, a rectangular FR-4 substrate is selected as the foundation due to its low cost, ease of availability, and suitability for prototype fabrication. This substrate provides the mechanical support for the antenna and plays a crucial role in determining its electrical performance. In the first stage, a simple rectangular patch is designed on the substrate, which serves as the baseline structure for further modifications and enhancements. The patch dimensions are determined using well-established design equations to ensure that the antenna operates within the desired frequency range. To achieve accurate performance, a detailed parametric analysis of both the radiating element and the ground structure was conducted, guided by the standard design relations as expressed in equations (1) to (6) [16–24]. These equations form the foundation for optimizing critical antenna parameters such as width, length, and effective dielectric constant. Among them, the patch width (W) is a fundamental parameter, as it directly influences the input impedance, radiation efficiency, and resonant frequency of the antenna. The patch width is calculated using the following basic expression:

$$W = \frac{c}{2f}\sqrt{\frac{2}{\varepsilon_{r+1}}} \tag{1}$$

Here, ε_r denotes the dielectric constant of the substrate, while f represents the center resonant frequency of the antenna. Once the patch width is obtained, the effective length of the patch is determined using the corresponding design relation. The actual length of the patch is then calculated by incorporating the fringing field effects, which are significant at the edges of the patch. The length of the patch can thus be expressed as:

$$L = L_{ef} - 2\Delta l \tag{2}$$

$$L_{ef} = \frac{c}{2f\sqrt{\varepsilon_{re}}} \tag{3}$$

Here, L_{ef} represents the effective length of the patch, while ε_{re} denotes the effective dielectric constant of the substrate, which can be expressed as:

$$\varepsilon_{re} = \frac{\varepsilon_{re}+1}{2} + \frac{\varepsilon_r - 1}{2}\left[1 + \frac{12h}{W}\right]^{-1/2} \tag{4}$$

Where, h is the thickness of substrate and the normalized extension in length (Δl) is given by:

$$\Delta l = 0.412\, h \frac{(\varepsilon_{re} + 0.3)\left(\frac{W}{h} + 0.8\right)}{(\varepsilon_{re} - 0.25\ B)\left(\frac{W}{h} + 0.8\right)} \tag{5}$$

Feed line length (L_f) is considered by using below equation.

$$L_f = \lambda_g/2 \tag{6}$$

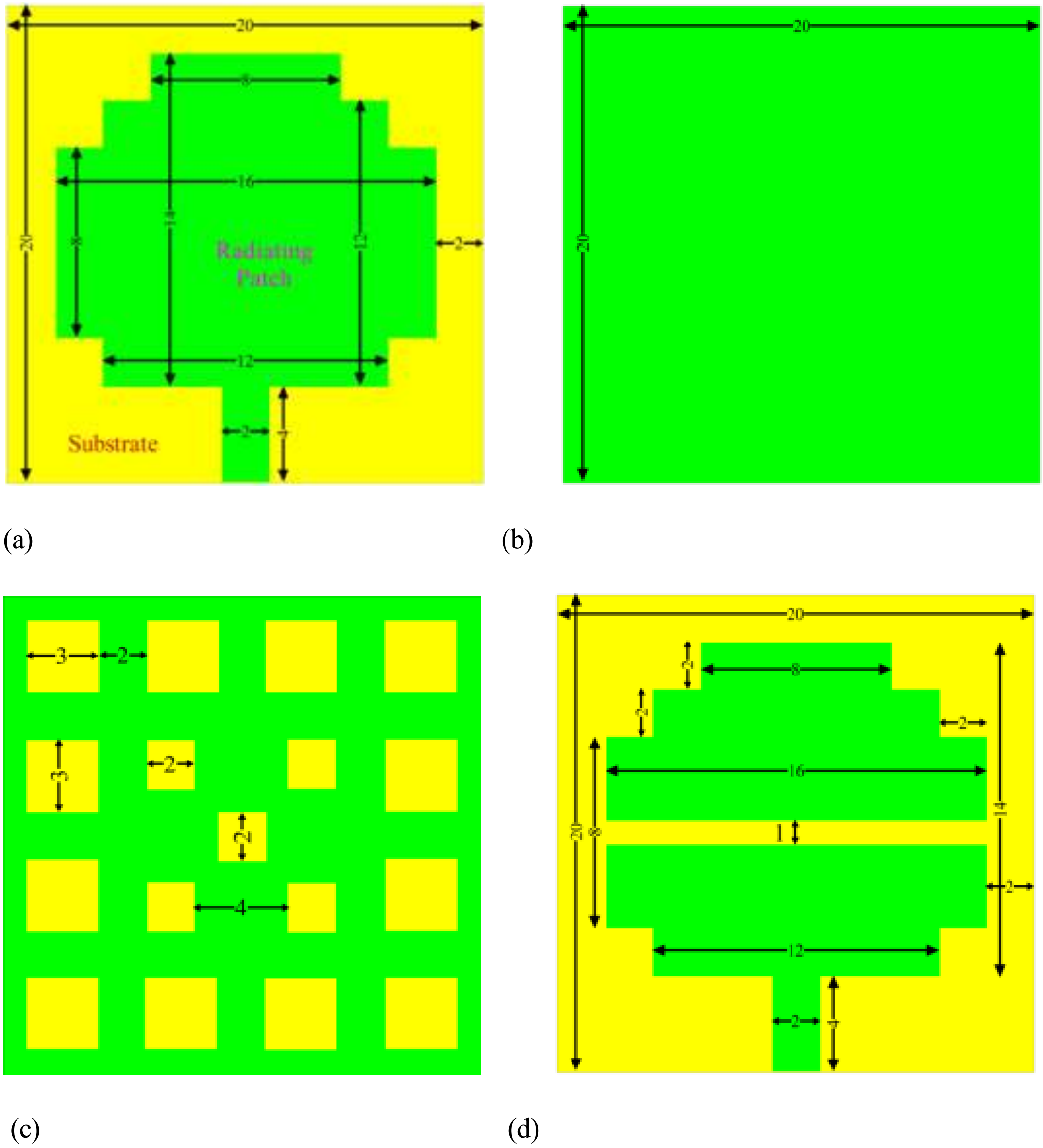

Fig. 2: Schematic representation of the proposed antenna: (a) Simple microstrip patch antenna, (b) corresponding plain ground plane, (c) fractal ground plane with square-shaped slots, and (d) radiating patch with PIN diode in OFF-state condition. [All dimensions are in millimeters]

The proposed microstrip patch antenna, illustrated in Fig. 2, is designed on a cost-effective FR4-epoxy substrate with a thickness of 1.6 mm and a relative permittivity of 4.4. The radiating patch is excited through a thin microstrip-line feed [18], with the feed line dimensions optimized to a length of 4 mm and a width of 2 mm for proper impedance matching. The overall antenna structure measures 20 × 20 mm2. Initially, a simple microstrip patch with a plain ground plane, as shown in Fig. 2(b), is considered. To improve performance, the ground plane is modified into a defective ground structure (DGS) by etching square-shaped fractal slots, as depicted in Fig. 2(c). The first iteration introduces square slots of 3 × 3 mm2, followed by a scaled-down version of 2 × 2 mm2 slots distributed on the ground plane. In the final stage, an additional 2 × 2 mm2 slot is etched at the center of the ground plane, completing the fractal slot configuration.

Furthermore, the reconfigurability of the antenna is achieved by incorporating a PIN diode into the radiating patch. As shown in Fig. 2(d), an 8 × 1 mm slot is introduced in the middle portion of the patch, representing the PIN diode OFF-state condition. This configuration satisfies the reconfigurable design criteria and enables the antenna to achieve multiband operation, making it suitable for modern wireless communication applications.

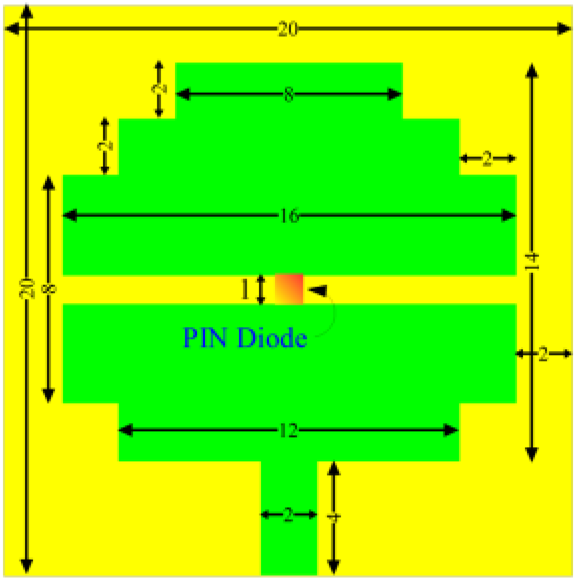

Fig. 3: Schematic diagram of the proposed antenna design with the PIN diode in the ON-state configuration. [Dimensions are given in millimeters]

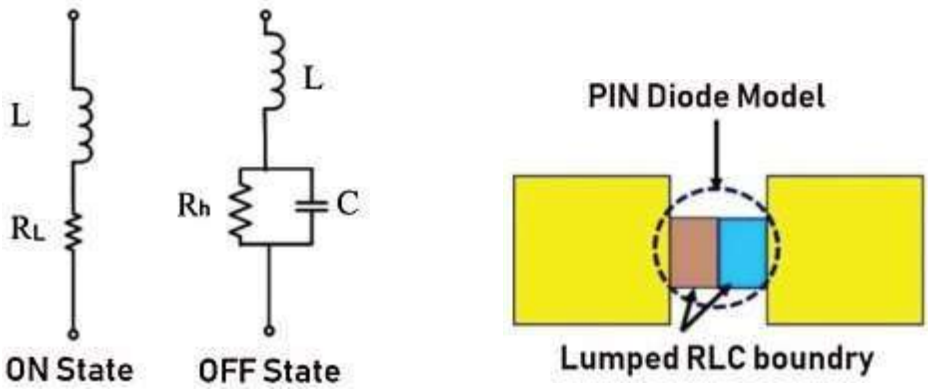

(a) (b)

Fig. 4: Equivalent RLC circuit representation of the proposed antenna: (a) illustrating the electrical characteristics of the integrated PIN diode under ON and OFF states, and (b) depicting the PIN diode model and its contribution towards achieving antenna reconfigurability.

The final geometry of the proposed antenna is derived from the initially designed plain ground structure, which is further modified into a fractal ground plane to enhance performance characteristics. For achieving reconfigurability, a single PIN diode is employed as the switching element. The diode is strategically positioned at the center of a rectangular slot etched on the radiating patch, as illustrated in Fig. 3. In this design, the PIN diode is modeled in HFSS with physical dimensions of 1 mm × 1 mm, based on the technical specifications provided in the datasheet of the Skyworks SMP1340 series, a surface-mountable PIN diode [21]. The electrical behavior of the diode is represented by its equivalent RLC

circuit, exhibiting distinct characteristics in the OFF and ON states, as depicted in Fig. 4(a) and Fig. 4(b), respectively. This switching mechanism enables reliable control over the current distribution within the patch, thereby facilitating dynamic frequency reconfiguration for multiband operation.
The equivalent circuit modeling of the PIN diode accounts for its distinct electrical behavior in the conducting (ON) and non-conducting (OFF) states. In the ON state, the diode is approximated as a short circuit, represented by a series combination of inductance (L_s) and resistance (R_s). Conversely, in the OFF state, the diode behaves as an open circuit and is modeled by a parallel combination of resistance (R_p) and capacitance (C_p), connected in series with the same inductance (L_s). For accurate simulation, the model values considered are: series inductance L_s=0.7 nHL in both ON and OFF states, series resistance R_s =1.2 Ω in the ON state, and for the OFF state, a parallel combination of capacitance C_p = 0.3pF and resistance R_p =5 MΩ [8–15]. This equivalent circuit representation effectively captures the switching characteristics of the diode, thereby enabling precise modeling of antenna reconfigurability.

3. RESULTS AND DISCUSSION

The proposed antenna was designed and simulated using the HFSS (High-Frequency Structure Simulator) tool, which employs the Finite Element Method (FEM) to discretize the computational domain into smaller mesh elements for accurate field analysis. The simulation outcomes are analyzed in this section. It is observed that adopting a discrete frequency sweep provides higher accuracy compared to a continuous sweep, while also reducing both computational time and memory requirements. The obtained results are further examined in terms of the antenna's performance parameters and radiation characteristics.
Figure 5(a) along with Table 1 presents a comparative analysis between the plain ground geometry and the fractal ground geometry of the proposed antenna. For the plain ground antenna, the operating bands were achieved at 8.38aaa–9.02 GHz (resonating at 8.81 GHz), 9.65–10.50 GHz (resonating at 10.07 GHz), and 15.35–16.83 GHz (resonating at 15.98 GHz). The corresponding peak gains were 2.36 dBi, 7.75 dBi, and 6.08 dBi, respectively, as illustrated in Fig. 6(a) and summarized in Table 1.
Furthermore, the performance of the proposed reconfigurable antenna under ON and OFF switching states of the PIN diode is analyzed in Fig. 5(b) and Table 1. In the OFF-state, the antenna exhibits operating bands of 7.96–8.38 GHz (resonating at 8.17 GHz), 10.92–11.55 GHz (resonating at 11.13 GHz), and 14.72–19.36 GHz (resonating at 15.77 GHz and 17.46 GHz). The corresponding peak gains achieved in this state are 9.12 dBi, 5.62 dBi, 8.75 dBi, and 7.61 dBi, respectively, across the resonant bands.
In contrast, the fractal ground plane antenna demonstrated a remarkable improvement in performance compared to the conventional plain ground configuration. The fractal geometry exhibited operating bands at 8.38–9.02 GHz (resonating at 8.60 GHz), 9.65–10.28 GHz (resonating at 9.86 GHz), and 14.72–17.67 GHz (resonating at 15.35 GHz). The corresponding peak gains were observed as 5.61 dBi, 2.28 dBi, and 13.87 dBi, respectively, as illustrated in Fig. 6(a) and detailed in Table 1. This comparative analysis clearly indicates that the fractal ground geometry offers superior gain and enhanced bandwidth in comparison to the plain ground configuration, thereby validating the effectiveness of employing fractal structures in ground plane design for optimized antenna performance in modern wireless communication systems.

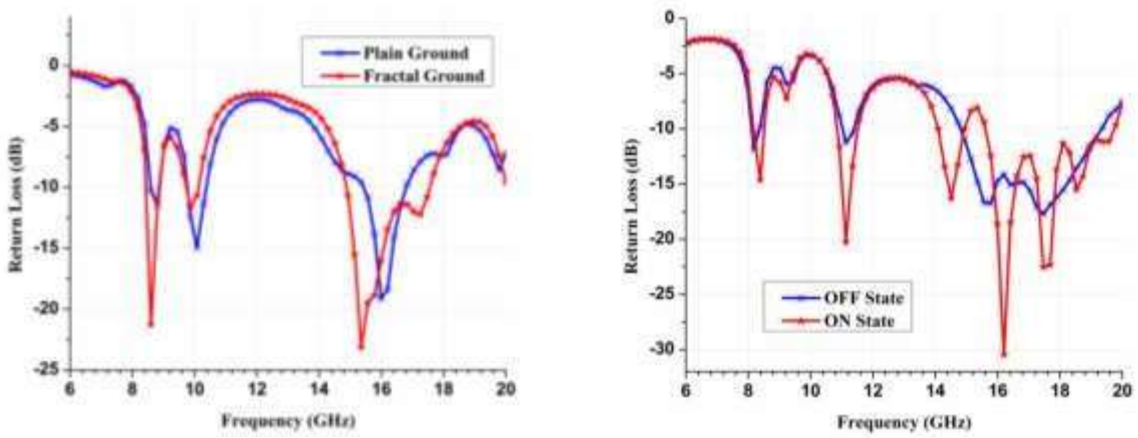

(a) (b)

Fig. 5: Variation of the simulated $|S_{11}|$ parameter with frequency for all design configurations of the proposed antenna, highlighting the resonant frequencies and impedance matching behavior under different structural and reconfigurable conditions.

Table 1: Simulated performance metrics of the antenna for different ground geometries

Antenna Geometries	Operating Band (GHz)	Resonant Frequency (GHz)	Return Loss (dB)	Peak Gain (dBi)	Radiation Efficiency (%)	VSWR
Plain Ground	8.38-9.02	8.81	-11.49	2.36	72.50	1.07
	9.65-10.50	10.07	-14.93	7.75	65.40	1.52
	15.35-16.83	15.98	-19.14	6.08	57.07	1.62
Fractal Ground	8.38-9.02	8.60	-21.24	5.61	71.80	1.62
	9.65-10.28	9.86	-11.66	2.28	66.50	1.92
	14.72-17.67	15.35	-23.12	13.87	61.80	1.23
Reconfigurable OFF-State	7.96-8.38	8.17	-11.85	9.12	71.13	1.44
	10.92-11.55	11.13	-11.22	5.62	85.43	1.20
	14.72-19.36	15.77	-16.72	8.75	75.63	1.58
		17.46	-17.71	7.61	77.90	1.93
Reconfigurable ON-State	7.96-8.60	8.38	-14.62	13.30	80.96	1.52
	10.71-11.55	11.13	-20.25	4.67	85.43	1.47
	14.08-15.14	14.51	-16.29	13.17	73.36	1.05
	15.56-19.78	16.20	-30.44	9.92	88.16	1.75
		17.46	-22.52	7.91	86.78	1.15
		18.52	-15.50	14.55	79.03	1.95

In the ON-state, the antenna achieves broader operating bands of 7.96–8.60 GHz (resonating at 8.38 GHz), 10.71–11.55 GHz (resonating at 11.13 GHz), 14.08–15.14 GHz (resonating at 14.51 GHz), and 15.56–19.78 GHz (resonating at 16.20 GHz, 17.46 GHz, and 18.52 GHz). The corresponding peak gains in this state are recorded as 13.30 dBi, 4.67 dBi, 13.17 dBi, 9.92 dBi, 7.91 dBi, and 14.55 dBi, confirming substantial enhancement in performance under reconfiguration (c.f. Fig. 6(b) and Table 1).

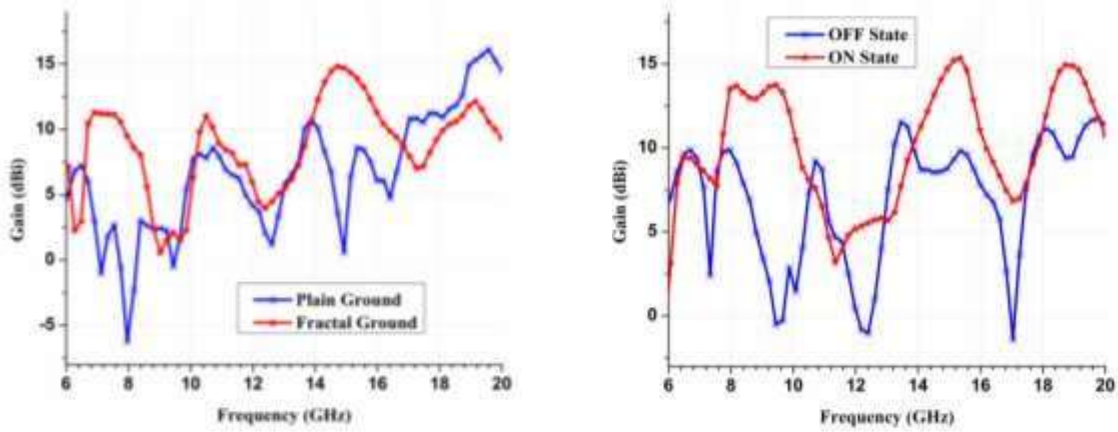

(a) (b)

Fig. 6: Simulated variation of the gain with respect to frequency for all design configurations of the proposed antenna, illustrating the performance differences across plain ground, fractal ground, and reconfigurable ON/OFF states of the PIN diode.

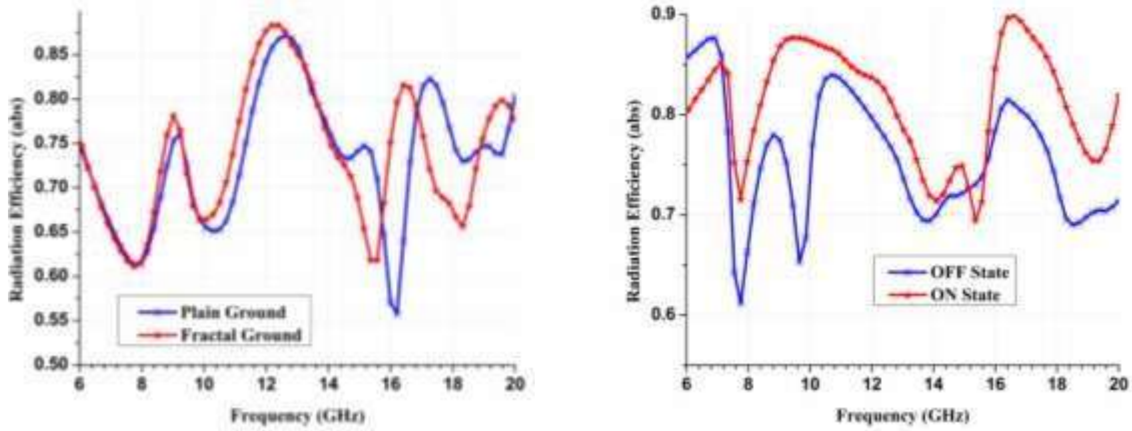

(a) (b)

Fig. 7: Simulated variation of radiation efficiency with respect to frequency for the complete antenna configurations, highlighting the comparative performance of plain ground, fractal ground, and PIN diode ON/OFF switching states of the proposed reconfigurable design.

It is further observed that the S11 parameter remains well below –10 dB for both ON and OFF switching states of the PIN diode, ensuring effective impedance matching. Moreover, the radiation efficiency characteristics of the antenna are depicted in Fig. 7(a) for plain and fractal ground geometries and in Fig. 7(b) for the ON and OFF states of the reconfigurable antenna. The results indicate that the antenna consistently maintains satisfactory radiation efficiency across all operating conditions, thereby demonstrating its suitability for high-performance reconfigurable wireless systems.

International Journal of Environmental Sciences
ISSN: 2229-7359
Vol. 10 No. 6s,2024
https://theaspd.com/index.php

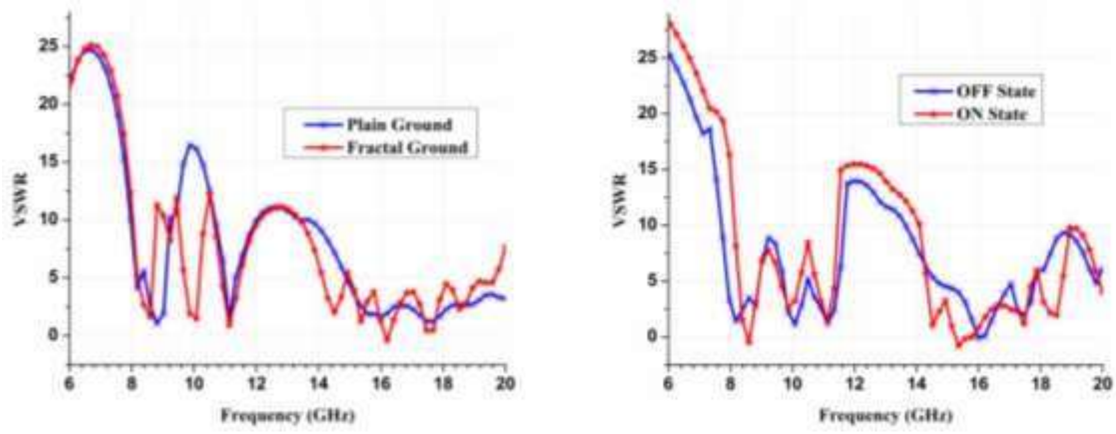

(a) (b)

Fig. 8: Variation of VSWR with frequency for the complete antenna design, illustrating performance under plain and fractal ground configurations as well as ON/OFF switching states of the PIN diode.

The VSWR characteristics of the proposed antenna are illustrated in Fig. 8(a) and Fig. 8(b), corresponding to the plain/fractal ground configurations and the ON/OFF switching states of the PIN diode, respectively. In both cases, the VSWR remains consistently below the acceptable limit of 2 across all resonant frequencies, ensuring proper impedance matching and stable antenna performance. Furthermore, the variation of peak gain (in dBi) across the operating frequency bands is shown in Fig. 5, which clearly demonstrates the improved radiation characteristics enabled by the proposed design. The antenna attains a maximum gain of 14.55 dBi at 18.52 GHz, thereby confirming its suitability for high-gain wireless applications. A comprehensive summary of the antenna's resonant frequencies, return loss, VSWR, gain, and radiation efficiency is provided in Table 1. These results exhibit strong consistency across all operating bands, thereby validating the effectiveness and reliability of the proposed design.

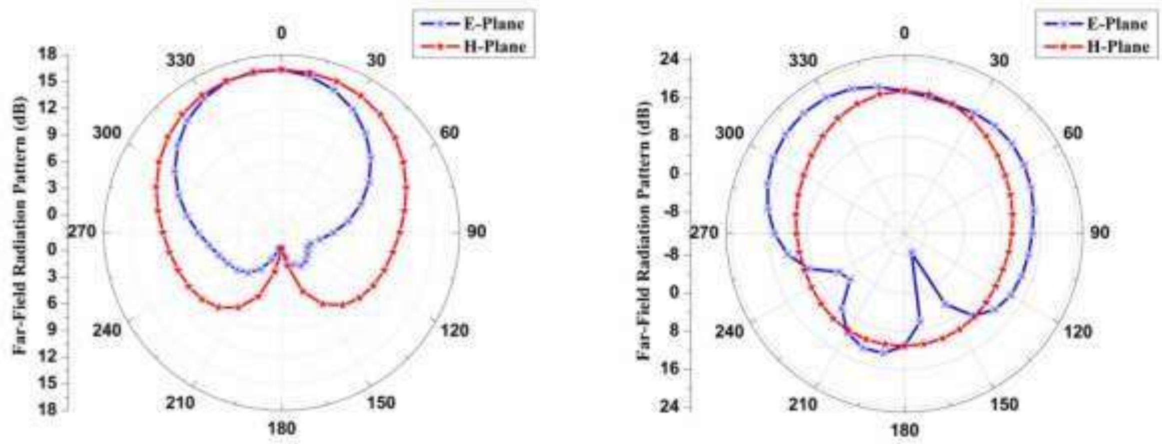

(a) (b)

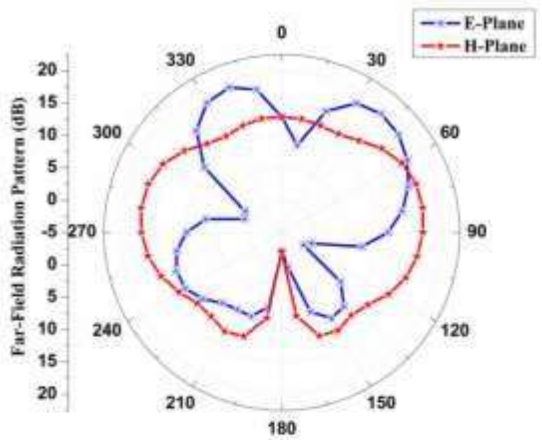

E-Plane
H-Plane
Far-Field Radiation Pattern (dB)
0
30
60
90
120
150
180
210
240
270
300
330

(c)

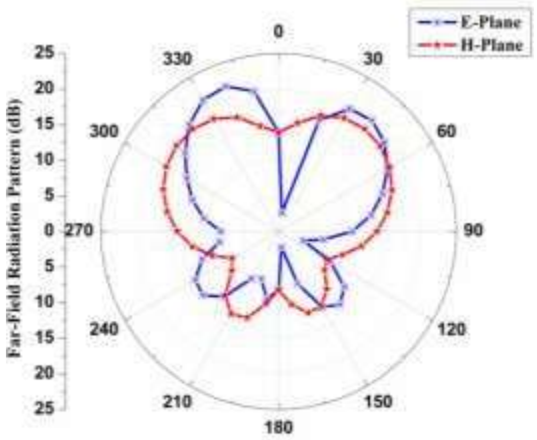

E-Plane
H-Plane
Far-Field Radiation Pattern (dB)
0
30
60
90
120
150
180
210
240
270
300
330

(d)

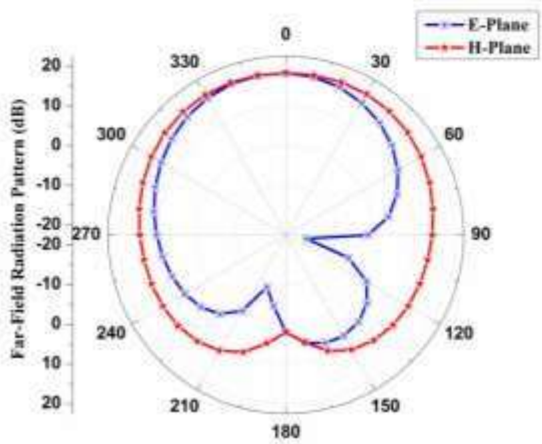

E-Plane
H-Plane
Far-Field Radiation Pattern (dB)
0
30
60
90
120
150
180
210
240
270
300
330

(e)

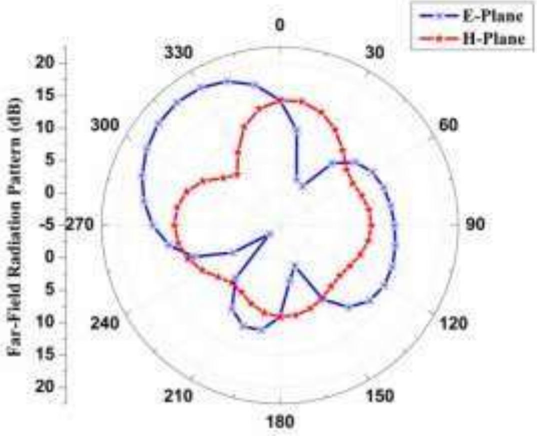

E-Plane
H-Plane
Far-Field Radiation Pattern (dB)
0
30
60
90
120
150
180
210
240
270
300
330

(f)

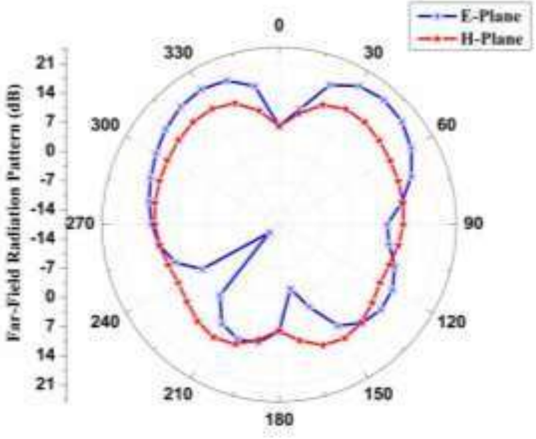

E-Plane
H-Plane
Far-Field Radiation Pattern (dB)
0
30
60
90
120
150
180
210
240
270
300
330

(g)

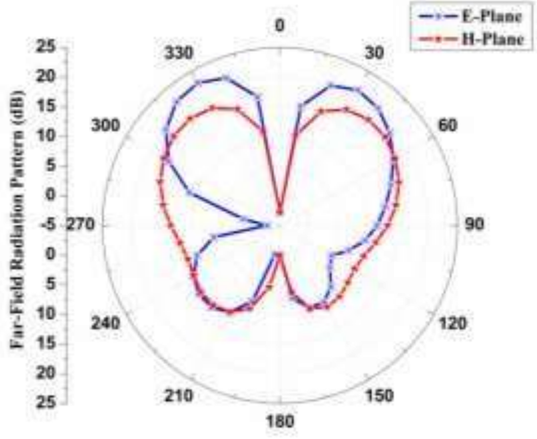

E-Plane
H-Plane
Far-Field Radiation Pattern (dB)
0
30
60
90
120
150
180
210
240
270
300
330

(h)

International Journal of Environmental Sciences
ISSN: 2229-7359
Vol. 10 No. 6s,2024
https://theaspd.com/index.php

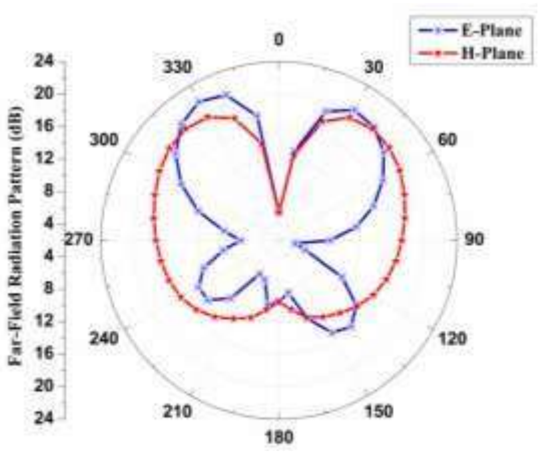

(i)

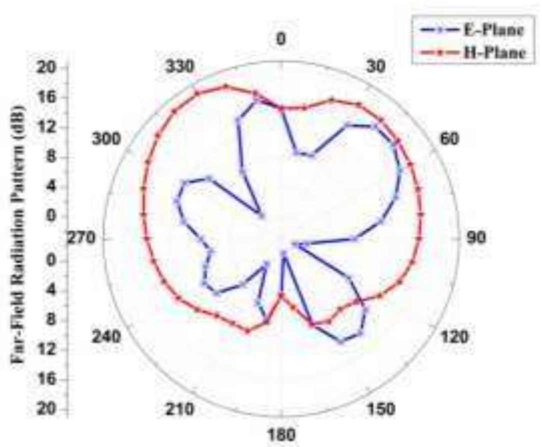

(j)

Fig. 9: Radiation patterns of the proposed antenna under PIN diode switching conditions. The OFF-state configurations correspond to resonant frequencies at (a) 8.17 GHz, (b) 11.13 GHz, (c) 15.77 GHz, and (d) 17.46 GHz, while the ON-state configurations correspond to resonant frequencies at (e) 8.38 GHz, (f) 11.13 GHz, (g) 14.51 GHz, (h) 16.20 GHz, (i) 17.46 GHz, and (j) 18.52 GHz.

Table 2: Benchmarking of the proposed antenna against reported designs in literature

Ref.	No of Band	Antenna Size (mm^3)	Operating Band (GHz)	Antenna Gain (dBi)	VSWR	Radiation Efficiency (%)
[11]	2	35×30×1.6	11.35-12.02 13.54-14.30	4.67 3.55	3.96 2.64	NR
[13]	3	28×28×1.57	10.65-12.50 14.68-15.85 17.34-18.32	2.42 1.65 3.64	NR	65.40
[17]	2	70×70×1.6	6.38-9.32 11.55-12.74	2.78 4.87	NR	NR
[18]	2	40×30×1.6	9.65-10.28 14.64-15.76	3.71 2.78	4.52 1.86	72.54
[19]	2	30×30×1.6	13.76-14.67 15.86-16.97	2.95 5.82	NR	NR
[21]	2	30×25×1.57	12.94-13.38 14.94-16.65	3.86 2.75	1.98 2.71	NR
Proposed	**4**	**20×20×1.6**	**07.96-08.60** **10.71-11.55** **14.08-15.14** **15.56-19.78**	**13.30** **04.67** **13.17** **14.55**	**1.52** **1.47** **1.05** **1.95**	**80.96** **85.43** **73.36** **79.03**

The far-field behavior of the antenna is further examined through its radiation patterns, which provide a graphical representation of the antenna's directional radiation properties. Fig. 9(a–d) illustrates the radiation patterns for the OFF-state condition of the PIN diode, corresponding to resonant frequencies at 8.17 GHz, 11.13 GHz, 15.77 GHz, and 17.46 GHz. In contrast, Fig. 9(e–j) depicts the radiation patterns under the ON-state condition, with resonances at 8.38 GHz, 11.13 GHz, 14.51 GHz, 16.20 GHz,

17.46 GHz, and 18.52 GHz. These results confirm that the proposed reconfigurable antenna maintains desirable radiation performance across both diode switching states.
The E-plane corresponds to φ = 0°, while the H-plane corresponds to φ = 90° for the proposed antenna's radiation patterns. The simulated radiation characteristics at the respective resonant frequencies exhibit stable and directional behavior, ensuring consistent performance across the operating bands. Furthermore, the obtained results demonstrate that the antenna maintains good gain and well-defined radiation patterns, making it highly suitable for a wide range of modern wireless and communication applications.
Table 2 presents a comparative evaluation of the proposed antenna design with previously reported works in terms of the number of operating bands, antenna size, frequency range, peak gain, voltage standing wave ratio (VSWR), and radiation efficiency. The results indicate that the proposed antenna not only achieves satisfactory performance but also demonstrates strong potential for practical applications. In comparison with the designs reported in [11], [13], [17], [18], [19], and [21], the proposed antenna exhibits a more compact size, while simultaneously offering enhanced performance metrics. Notably, both the peak gain and radiation efficiency are significantly improved, underscoring the superiority and effectiveness of the proposed design over existing literature.

4. CONCLUSION

In this work, a novel antenna design has been presented that effectively integrates fractal geometry with frequency reconfiguration capability, thereby achieving a remarkable enhancement in overall performance. The proposed structure leverages the advantages of fractal-based miniaturization and multiband characteristics, along with the reconfigurability offered by a PIN diode, enabling dynamic switching between multiple resonant bands. Designed on a cost-effective FR4-epoxy substrate and employing a simple microstrip feed line; the antenna ensures ease of fabrication and reduced implementation cost without compromising performance. The antenna demonstrates reliable frequency agility across the X-band and Ku-band, exhibiting stable impedance matching, improved gain, and satisfactory radiation efficiency under both ON and OFF switching states. Such versatility makes the proposed design highly suitable for modern and emerging wireless applications, including vehicular communication systems, satellite communication, radar systems, and advanced reconfigurable wireless networks. The results validate that the integration of fractal geometry with reconfigurable techniques can serve as a promising approach to develop compact, cost-efficient, and high-performance antennas for next-generation communication technologies.

REFERENCE

[1] M. K. Shereen, M. I. Khattak, and J. Nebhen, "A review of achieving frequency reconfiguration through switching in microstrip patch antennas for future 5G applications," Alexandria Engineering Journal, vol. 61, no. 1, pp. 29–40, 2022.
[2] M. Ikram, N. Nguyen-Trong, and A. Abbosh, "A simple single-layered continuous frequency and polarization-reconfigurable patch antenna array," IEEE Trans. Antennas Propag., vol. 68, no. 6, pp. 4991–4996, 2019.
[3] S. Xiao, B. Z. Wang, and X. S. Yang, "A novel frequency-reconfigurable patch antenna," Microwave and Optical Technology Letters, vol. 36, no. 4, pp. 295–297, 2003.
[4] A. M. Yadav, C. J. Panagamuwa, and R. D. Seager, "Investigating the effects of control lines on a frequency reconfigurable patch antenna," Proc. Loughborough Antennas & Propagation Conf., pp. 605–608, Nov. 2010.
[5] W. H. Weedon, W. J. Payne, and G. M. Rebeiz, "MEMS-switched reconfigurable antennas," Proc. IEEE APS Int. Symp., vol. 3, pp. 654–657, Jul. 2001.
[6] H. T. Chattha, M. Hanif, X. Yang, I. E. Rana, and Q. H. Abbasi, "Frequency reconfigurable patch antenna for 4G LTE applications," Progress In Electromagnetics Research M, vol. 69, pp. 1–13, 2018.
[7] X. Zhang, X. Zou, X. Lu, C. W. Tang, and K. M. Lau, "Fully- and quasi-vertical GaN-on-Si PIN diodes: High performance and comprehensive comparison," IEEE Trans. Electron Devices, vol. 64, no. 3, pp. 809–815, 2017.
[8] M. Shirazi, T. Li, and X. Gong, "Effects of PIN diode switches on the performance of reconfigurable slot-ring

antenna," Proc. IEEE WAMICON, pp. 1–3, Apr. 2015.

[9] P. Thanki and F. Raval, "I-shaped frequency and pattern reconfigurable antenna for WiMAX and WLAN applications," Progress In Electromagnetics Research Lett., vol. 97, pp. 149–156, 2021.

[10] A. K. Saroj and J. A. Ansari, "A reconfigurable multiband rhombic shaped microstrip antenna for wireless smart applications," Int. J. RF and Microwave Computer-Aided Engineering, vol. 30, p. e22378, Oct. 2020.

[11] M. Borhani, P. Rezaei, and A. Valizade, "Design of a reconfigurable miniaturized microstrip antenna for switchable multiband systems," IEEE Antennas Wireless Propag. Lett., vol. 15, pp. 822–825, Sep. 2015.

[12] M. Jenath and V. Nagarajan, "Review on frequency reconfigurable antenna for wireless applications," Proc. Int. Conf. on Communication and Signal Processing (ICCSP), pp. 2240–2245, Apr. 2017.

[13] L. Han, C. Wang, X. Chen, and W. Zhang, "Compact frequency-reconfigurable slot antenna for wireless applications," IEEE Antennas Wireless Propag. Lett., vol. 15, pp. 1795–1798, Mar. 2016.

[14] L. Han, C. Wang, W. Zhang, R. Ma, and Q. Zeng, "Design of frequency- and pattern-reconfigurable wideband slot antenna," Int. J. Antennas and Propagation, vol. 2018, pp. 1–9, Feb. 2018.

[15] H. F. Abutarboush and A. Shamim, "A reconfigurable inkjet-printed antenna on paper substrate for wireless applications," IEEE Antennas Wireless Propag. Lett., vol. 17, pp. 1648–1651, Jul. 2018.

[16] H. Dholakiya, D. Pujara, and S. B. Sharma, "Wide-slot fractal antenna design with improved bandwidth," Proc. IEEE AEMC, pp. 1–3, 2011.

[17] W. Chen, G. Wang, and C. Zhang, "Small-size microstrip patch antennas combining Koch and Sierpinski fractal shapes," IEEE Antennas Wireless Propag. Lett., vol. 7, pp. 738–741, 2008.

[18] H. Oraizi and S. Hedayati, "Miniaturized UWB monopole microstrip antenna design by the combination of Giuseppe Peano and Sierpinski carpet fractals," IEEE Antennas Wireless Propag. Lett., vol. 10, pp. 67–70, 2011.

[19] A. Farswan, A. K. Gautam, B. K. Kanaujia, and K. Rambabu, "Design of Koch fractal circularly polarized antenna for handheld UHF RFID reader applications," IEEE Trans. Antennas Propag., vol. 64, no. 2, pp. 771–775, Feb. 2016.

[20] Y. Cai, K. Li, Y. Yin, S. Gao, W. Hu, and L. Zhao, "A low-profile frequency reconfigurable grid-slotted patch antenna," IEEE Access, vol. 6, pp. 36305–36312, 2018.

[21] S. S. Yang, A. A. Kishk, and K. Lee, "Frequency reconfigurable U-slot microstrip patch antenna," IEEE Antennas Wireless Propag. Lett., vol. 7, pp. 127–129, 2008.

[22] H. A. Majid, M. K. A. Rahim, M. R. Hamid, N. A. Murad, and M. F. Ismail, "Frequency-reconfigurable microstrip patch-slot antenna," IEEE Antennas Wireless Propag. Lett., vol. 12, pp. 218–220, 2013.

[23] H. Gu, J. Wang, L. Ge, and C. Sim, "A new quadri-polarization reconfigurable circular patch antenna," IEEE Access, vol. 4, pp. 4646–4651, 2016.

[24] W. Li, Y. M. Wang, Y. Hei, B. Li, and X. Shi, "A compact low-profile reconfigurable metasurface antenna with polarization and pattern diversities," IEEE Antennas Wireless Propag. Lett., vol. 20, no. 7, pp. 1170–1174, Jul. 2021.

[25] A. K. Saroj and J. A. Ansari, "A reconfigurable multiband rhombic shaped microstrip antenna for wireless smart applications," International Journal of RF and Microwave Computer-Aided Engineering, vol. 30, p. e22378, Oct. 2020.

[26] M. Ikram, N. Nguyen-Trong, and A. Abbosh, "A simple single-layered continuous frequency and polarization-reconfigurable patch antenna array," IEEE Transactions on Antennas and Propagation, vol. 68, no. 6, pp. 4991–4996, 2019.

[27] J. S. Petko and D. H. Werner, "Miniature reconfigurable three-dimensional fractal tree antennas," IEEE Trans. Antennas Propag., vol. 52, no. 8, pp. 1945–1956, Aug. 2004.

[28] J. T. Rayno and S. K. Sharma, "Frequency reconfigurable spirograph planar monopole antenna (SPMA)," Proc. Int. Symp. on Antennas and Propagation (ISAP), pp. 1305–1308, 2012.

[29] T. Al-Maznaee and H. E. Abd-El-Raouf, "Design of reconfigurable patch antenna with a switchable V-slot," Proc. Asia-Pacific Conf. on Applied Electromagnetics, pp. 1–5, Dec. 2007.